This article has been accepted for publication in a future issue of this journal, but has not been fully edited.
Content may change prior to final publication in an issue of the journal. To cite the paper please use the doi provided on the Digital Library page.

A 3D Printed Utility Dielectric Core Manufacturing Process for Antenna Prototyping.

J. A. Brister [1] and R. M. Edwards [1*]

[1] Mechanical, Electrical and Manufacturing Engineering, Loughborough University, England, UK
[*]r.m.edwards@lboro.ac.uk

Abstract: A prototyping method for dielectrically loaded antennas is presented. Dielectric loading has been used with horn antennas, feeds, and lenses. Dielectrics have also been used for coating antennas submerged in water and biological matter and have led to improvements in bandwidth and efficiency as well as antenna miniaturisation. In this paper, we present a new technique to produce variable dielectrics with permittivity from 6 to 28 using two commonly available powders, titanium dioxide (used in foods) and magnesium silicate (used in talcum powder). An example spherical helical ball antenna is used to demonstrate the process. In this antenna, the mixed powders were encased in a 3D printed shell that achieved a reduction in diameter of the spherical antenna by a factor of 1.85. The technique aids rapid prototyping and optimisation using search algorithms.

1. Introduction

Researchers have known for some time the benefits that dielectric loading can bring to their antenna designs. Dielectrically loaded antennas have been shown to have properties that are beneficial particularly for manipulating size and bandwidth.

However, high permittivity dielectrics may be difficult to realise in the sizes and shapes are that are needed. The authors of [1] sandwiched a flat twin arm printed spiral between two layers of dielectric and achieved a gain 6 dBi higher than a version without a dielectric cover. However, the antenna was not constructed. In [2] the team researched an eight-element twin layer dielectric rod antenna array having a 40% bandwidth at x-band with a gain of approximately 14 dBs. They concluded that a graded rod would have extended their work, but that manufacture was too expensive. Probe fed dielectric resonators made of high dielectric constant materials were looked at in [3]. A main finding of the work was to discover that high Q materials did not necessarily always lead to small bandwidth antennas and that in some cases dielectric resonator antennas could have greater bandwidth than their microstrip printed counterparts. A large set of numerical results were presented supported by few carefully selected measurements. The absence of measured results in many papers means it is reasonable to state that there is a need to simplify the prototyping of dielectrically loaded antennas. The method we present combines the flexibility of 3D printed moulds with dielectric cores of variable permittivity. The technique increases the range of antennas that can be created and also extends applications of existing antennas due to cheaper manufacture. We only consider non-magnetic in this paper and are therefore not concerned with permeability. However, the method could be extended to cover magnetic materials as well.

Currently the main techniques for making dielectrically loaded antenna prototypes use compressed sintered blocks, machined shaped blocks or powders. The desired electrical properties are fixed on order and, because the machining of ceramics is difficult, the process does not lend itself to tuning or parametrisation in a radio laboratory. In addition, prototype materials cannot be reused so precise and careful initial specifications are called for. The creation and machining of ceramics is done by a few specialist companies and is relatively expensive and takes time.

Another method involves the use of two-part setting mixed compounds. Once set the mixes cannot be reformed.

In the remainder of this paper, we present a technique that overcomes many of the problems of expense and inconvenience associated with the use of dielectrics for loading antennas.

The rest of this paper is laid out as follows: - Section 2 contains the analysis we have used to obtain the permittivity for our new combination of combined powders. Section 3 includes a discussion of powder-based high permittivity cores, the factors used to choose their components and how to measure their permittivity. In Section 4 the method we have used to measure the permittivity of the powders separately and combined is presented along with a chart of for core selection. To demonstrate the miniaturisation, use high permittivity cores, Section 5 shows a comparison between two similar antennas both with and without a compacted powder core. The 3D printing of core shells is contained in section 6. Section 7 consider the thickness of core and lastly, the conclusions for the paper are presented in section 7.

2. Analysis of the permittivity of a two Powder Mixture.

The author of [4] in work on coal mine fires was interested in the permittivity of dust. He considered the permittivity of mixtures of air, coal dust and limestone dust. The analysis used the Landau, Lifshitz and Louyenga (LLL) formula to calculate the complex permittivity as shown in Equation (1).

$$(\varepsilon_m)^{\frac{1}{3}} = v_1(\varepsilon_1)^{\frac{1}{3}} + v_2(\varepsilon_2)^{\frac{1}{3}} + v_3(\varepsilon_3)^{\frac{1}{3}} \qquad (1)$$

where $v_1 + v_2 + v_3 = 1$ (the unitary volume ratio)

In Equation 1, ε_m is the permittivity of the air and powder mixture and ε_1, ε_2 and ε_3 are the permittivities of air and the two powders respectively. Also, v_1, v_2 and v_2 are the volumes of the three dielectrics and these can be calculated using $v = m/\rho$ where $m =$ mass and $\rho =$ density.

The authors noted that uncompacted powders could have variable dielectric properties but, in this paper, we have extended the method to use compacted powder components with converged permittivity. In [4] the author also considered permittivity for coal dust constituted of dust and air. The permittivity is proportional to the cube roots of the volumes of air and coal.

We have extended this work to include calculation of the permittivity of two compacted powders. The compaction process removes most of the air so that the LLL formula now becomes

$$(\varepsilon_{core})^{\frac{1}{3}} = v_1(\varepsilon_1)^{\frac{1}{3}} + v_2(\varepsilon_2)^{\frac{1}{3}} \qquad (2)$$

where $v_1 + v_2 = 1$ (the unitary volume ratio for two powders)

In Equn. (2) ε_{core} is the permittivity of the powder mixture and ε_1, ε_2 are the permittivities of the two powders we have selected to create cores with values from 6 to 28.

3. Powder-based High Permittivity Cores.

3.1. Material selection

Two powders are needed to create a biphasic powder to form a core. The selection properties are shown in Table 1. In the table, the high permittivity powder is shown as high powder and the lower permittivity powder as low powder.

Table 1. Biphasic powder selection criteria for High Permittivity Cores

Parameter	Requirement	Reason
High Powder ε_r	High - ≥ maximum desired highest ε_r	Higher bound for the core @ 100% vol.
Low Powder ε_r	Low - ≤ minimum desired highest ε_r	Lower bound for the core @ 100% vol.
Tan δ	Low	Reduces losses, simplifies measurements
Availability	Commonly available in a consistent form	Reduces complexity in sourcing components.
Mechanical Properties	Poor	Allows crushing and compaction to remove pockets of air.
Relative Permeability	1 - Non-magnetic	Improves
Packing pressure before stable permittivity.	As low as possible	Reduces the mechanical strength needed in the 3D former.
Toxicity	Safe	Simplifies handling

In this paper, we have not considered permeability, but the technique could be adapted using magnetic materials such as iron filings. Many materials have different measured permittivity depending on their level of compaction and therefore need to be pressed before stable results can be obtained. In general, powder will converge in permittivity only after it has been crushed back into its solid form. To achieve this compaction the materials needed to have relatively poor mechanical strength.

According to the criteria in Table 1, three candidate substances were selected and researched. These were two grades of Titanium Dioxide TiO2 (anatase and rutile) and Magnesium Silicate (MgSiO3). The rutile form was discounted at an early stage and is discussed in the next section. Forms of Ti02 are known as high permittivity dielectrics, with low loss while MgSiO3 is known to have lower permittivity, again with low loss. Titanium Dioxide TiO2 (food additive grade E171) is a human-made form and is obtainable as a 40-micron powder for use as a food colouring additive [5]. It is registered as additive E171 for E.U. food inclusion and is widely available. Magnesium Silicate (MgSiO3) is used in Talcum Powder and is also widely available [5].

3.2 Dielectric Measurements

Dielectric measurements of powders are challenging. The open-ended coaxial probe method tried by S. O. Nelson and P.G. Bartley in [6] where the probe is dipped into the powder could not be used in this paper since our powders are compressed into a solid before the point of measurement. We have used an Agilent 2.5GHz split post resonator (N1501AE03), with an Anritsu VNA and a QWED Q meter [8] running on a desktop computer. Split post resonators require well machined solid laminar specimens with two strictly parallel faces and a thickness of 3mm. We placed our powders between two sheets of acetate to provide the 'well machined' surface which was

then passed through heavy parallel rollers. For both candidate powders, the complex permittivity was measured to be lower than the uncertainty of the instrument at or below 0.005. As well as a VNA, the split post resonator was also measured with a power meter and the same results were computed using the method of [7]. Due to their low loss, both Titanium Dioxide [9] TiO2 and Magnesium Silicate (MgSiO3) are used extensively in photovoltaic (PV) cell manufacture where efficiency is critical.

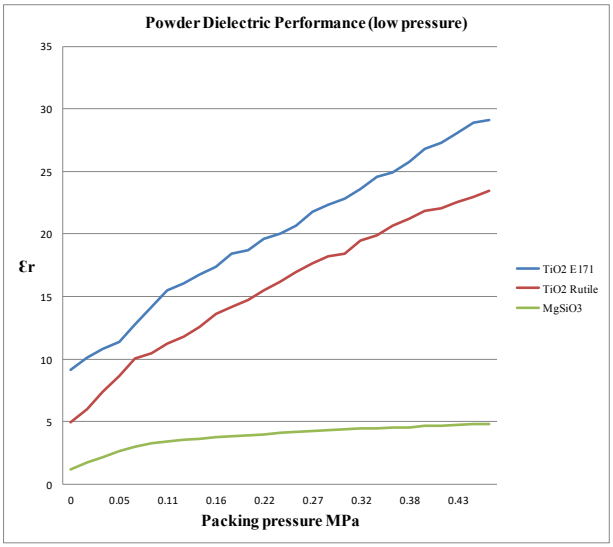

(a)

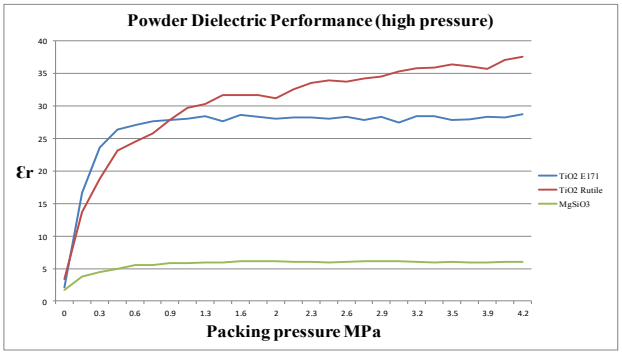

(b)

Fig. 1. *Dielectric vs Compaction Pressure for* ***(a)*** Low Pressure 60mm diameter test cell, ***(b)*** High Pressure 20mm diameter test cell.

In order to obtain the electrical properties of the high permittivity cores made of two mixed powders, two separate methods for dielectric characterisation were used. The first method obtained the permittivity of the powders as a function of compaction pressure and the second confirm the accuracy of the mixes predicted by Equation (2) when compared with measurements.

3.2.1 *Dielectric Measurements of Compacted Dielectric Single and Mixed Powders.*

There are two types of measurement required. The first stage is to coarsely characterise the starting materials concerning permittivity as a function of packing pressure, also noting the performance as the pressure was released to select an appropriate Standard Packing Pressure (SPP) for the intended use. This stage required a capacitance cell and a press.

For the second stage permittivity measurements were carried out for the powders compacted at SPP. This second stage validated the volumetric mixture described by Equation (2) and requires a resonant cavity and a press.

To measure the dielectric constant of a solid dielectric is to measure the capacitance of the material sandwiched between two parallel plates using the following equation.

$$C = k\varepsilon_0 \frac{A}{d} \qquad (3)$$

Where C, k, ε_0, A and d are the capacitance between the plates, the dielectric constant, the permittivity of free space, the area of the sample and the thickness of the sample respectively. Two cells were made with diameters of 20mm and

60mm and the plates forced together with bench press by controlled increments.

The results are shown in Figures 1 and 2. and show that below 4.2 MPa of pressure the Ti02 (rutile) did not converge to a stable permittivity but that at 1.5 MPa both Ti02 (anatase) and MgSi03 had done so. Therefore, these two materials were chosen as suitable powders. For these powders, we defined 1.5MPa as the minimum pressure for agglomeration. The acceptable examples have already flattened out below this pressure and do not change their permittivity when the small, but unavoidable kick-back occurs as the pressure is removed.

Table 2 presents the values for permittivity obtained using our measurements and Equation (3). Compressing the powders into a known volume and their weight allows their density to be computed. For the next stage, stage two, Equation

Table 2. Converged Permittivity of Compacted Powders at 1.5 MPa.

Material @ 1.5 MPa	ε_r	$\sqrt[3]{\varepsilon_r}$	Density g/c^3
Titanium Dioxide (E171)	28	3.036	1.065
Magnesium Silicate	6.09	1.827	1.067

2 was used to obtain the proportions of the powders predicted to make a mixed powder with a permittivity range of 6 to 28. To measure the dielectric constant of the mixed compacted powers a resonant cavity was designed in CST and then optimised to work with a QWED Q meter module [8] over 1.4 GHz to 2.6GHz.

A technique for making resonant cavities is proposed in [10] along with the relevant theory for deriving the permittivity from the S21 of the cavity as the presence of the sample changes its resonance.

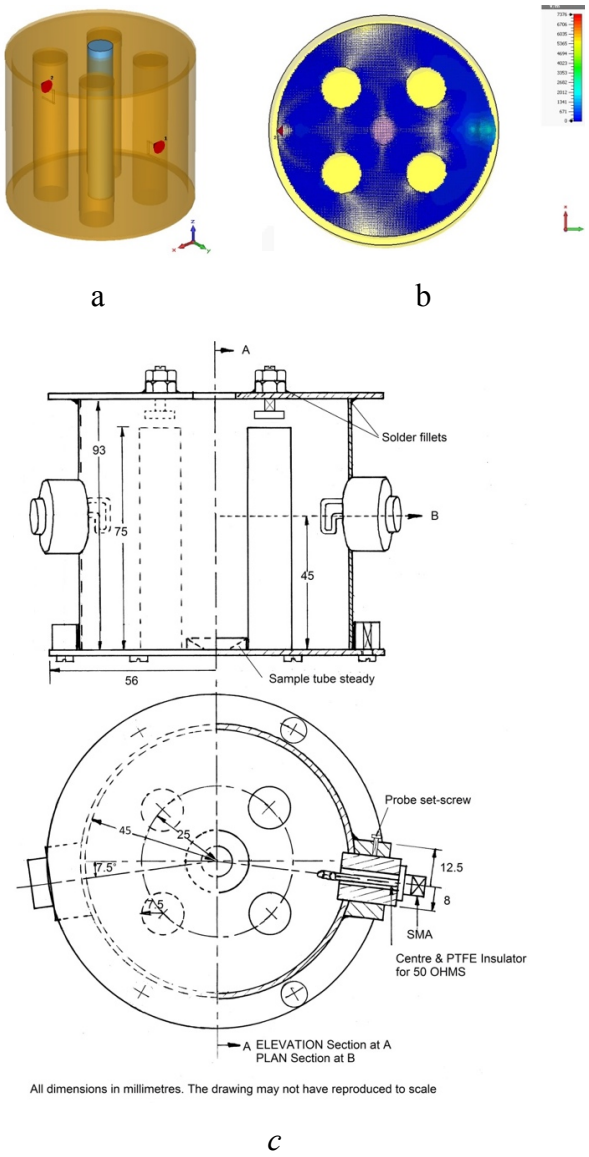

Fig. 2. Cavity Resonator for permittivity measurements of single or agglomerated powder dielectrics. ***(a) the CST geometry of the resonator. (b) Electric field with a sample in the model with dielectric Ɛr = 15 (c) shows the dimensions of the cavity resonator.***

In Figure 2 the CST model and the drawing of the copper cavity resonator built to measure the core powders are shown. For measurement, the powders, separate and mixed, are packed into the central tube created by a 3D printer.

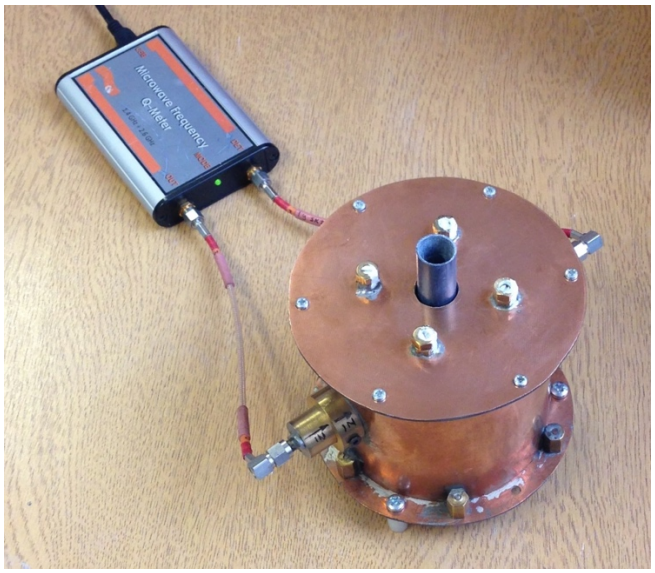

(a)

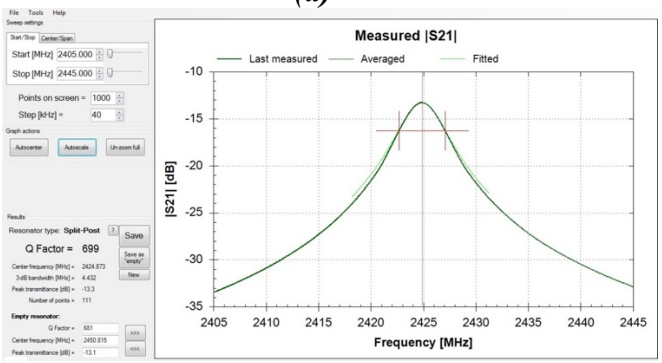

(b)

***Fig 3. (a) Cavity resonator built to measure powders – shown with a QWED Q meter [8]. (b) An example result after curve fitting. The real and complex parts of the permittivity are gathered from changes to the resonant frequency and Q respectively* [7, 8].**

Figure 3 shows the resonant cavity built to measure the powders used in this paper. Resonator measurements were calibrated against CST for a broad range of materials. Values for the two candidates are shown in Table 3.

Table 3. CST and Cavity values for permittivity.

Material	ε_r	CST Modelled results			Prototype Cavity Results		
		Resonant F. (MHz)	Q	Δf (MHz)	Resonant F. (MHz)	Q	Δf (MHz)
Empty	1	2248	875	0	2245.9	681	0
PTFE	2.2	2250	714	38	2411.5	530	34.5
MgSi03	6.2	2435	573	53	2406.8	551	41.3
Ti02	28	2330	733	118	2391.2	531	54.7

4. Single and Mixed Powder Results

Using the resonator, the results in Table 4 were obtained and compared with the predicted values obtained from the formula in Equation 2.

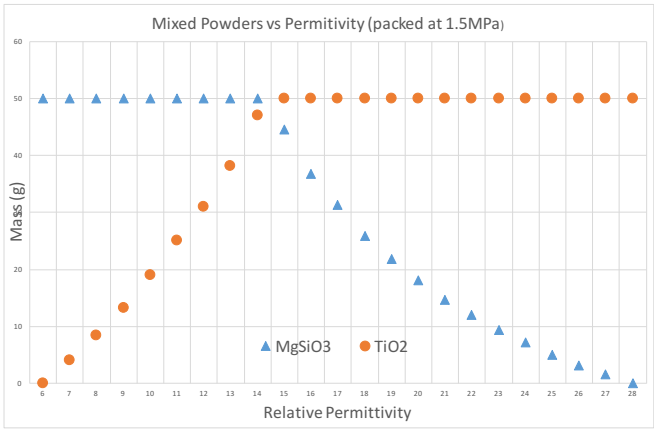

Figure 4. Compacted twin powder dielectric mixes for batches of 50g to 100g with relative permittivity of 6 to 28.

The complete range of proportions by weight for batches up to 100g is shown in Figure 4.

Table 4. Compacted twin powder dielectric mixes for batches of any required volume with relative permittivity of 7.5 to 25.

Unitary Volume ratios		Calculated and measured results		
TiO2	MgSiO3	LLL ε_r	Measured ε_r	Error %
0.1028	0.8972	7.5	7.1	-4
0.2574	0.7426	10	9.75	-2.5
0.3883	0.6117	12.5	12.2	-3
0.5027	0.4972	15	14.8	-2
0.605	0.395	17.5	17.35	-1.5
0.6976	0.3024	20	19.85	-1.5
0.7825	0.2174	22.5	22.4	-1
0.8632	0.1368	25	24.9	-1

Table 4 shows the proportions of powders used the make the mixed powders to the desired permittivity. The values predicted by Equation 2 are compared with the measured values. In this set of experiments, the maximum error value was found to be approximately 5%. The whole range of mixes is plotted in Figure 4. As an example for a dielectric constant of 10, 50g of MgSi03 should be mixed with 20g of Ti02 compacted to 1.5MPa.

5. High Permittivity Core - Comparison of an Air Cored and Dielectric Cored Spherical Helical Antenna

As has been described in the introduction of this paper, dielectric loading can offer several advantages to antenna design. The most important of these is the size reduction of antennas. Size reductions to the order of $\frac{1}{\sqrt{\varepsilon_r}}$ are possible or 1/5 for the permittivity range developed in this paper. To illustrate this last point, we designed, built and measured two generic antennas for operation at 2.2 GHz. One with an air core and one with a dielectric core. The design method can be found in [10], and typical patterns can be found in [11]. Details of the test antennas can be found in Figure 5 and Table 5. The method developed here is particularly well suited to optimisation of antenna designs using genetic algorithms in which an uninterrupted range of characteristics is desirable.

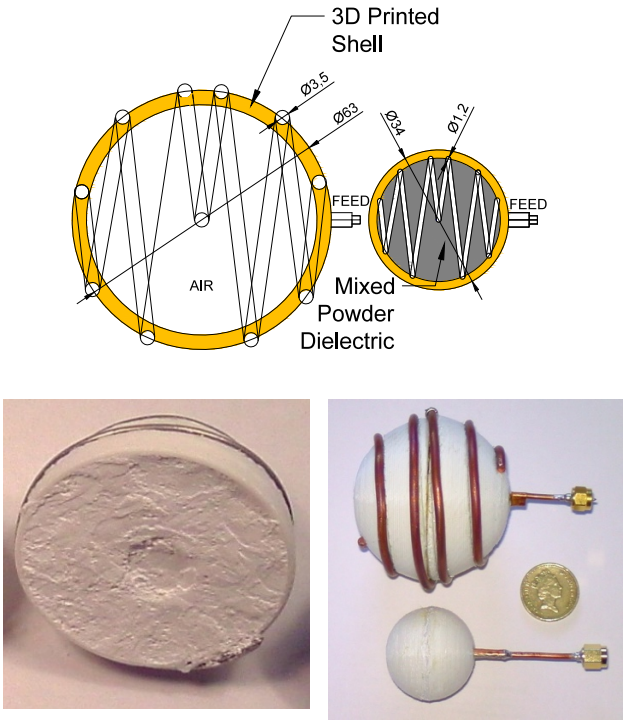

Figure 5. Structural Diagram and Photos of test antennas showing a reduction in size factor of 1.85. Bottom left shows the compacted powder.

Table 5. Parameters and results for the two test antennas shown in Figure 4.

Parameters	Air Cored	Powder
Shell diameter (mm)	63 ($0.46\lambda_0$)	34 ($0.25\lambda_0$)
Wire diameter (mm)	0.35 ($0.026\lambda_0$)	1.2 ($0.009\lambda_0$)
Number of turns	2.1	2.1
Shell Thickness (mm)	3.5 ($\varepsilon_r = 2.5$)	2.1 ($\varepsilon_r = 2.5$)
Wire position	Outer surface of Shell	Inner surface of shell
Fill	Air (ε_r=1)	Mixed Powder (ε_r = 15)
Volume (cm^3)	130.9	20.5
CST Simulated Results		
Centre frequency (MHz)	1960	2265
S_{11} at resonance	-5.5 dB	-22dB
3dB bandwidth	66 MHz (3%)	70 MHz (3%)
Measured Results		
Centre frequency	2285 MHz	2200 MHz
S_{11}	-5.5 dB	-23 dB
3dB width	65 MHz (3%)	60 MHz (3%)

6. 3D Printing Methods for Dielectrically Loaded antennas.

In our example, the printed 3D shell has two purposes. Firstly, to act as a mould to allow compacting of the two mixed powers and secondly to serve as a former for the thin wire antenna. In Figure 4 two antennas are shown, the larger is an air-filled ball antenna wound upon a 3.5mm thick shell containing a miniature balun and feed. The smaller is an antenna with a 2.1 mm thick shell and a dielectric core of ε_r=15. Both antennas were synthesised in CST for operation at 2.2 GHz. The thickness of the printed shell wall is a decision which must be taken early in the antenna design process. A thin wall is desirable as the shell either increases the overall dimensions (if it is added outside the core), or reduces the available volume (if it is subtracted from the core), for high dielectric materials in the finished prototype antenna. Our research suggests that 1.3 mm is the minimum thickness to withstand the packing pressures for the mixed powders used (Section 3). First, a 3D graphic STL file was output from the antenna

modelling software. A single hemisphere is shown in the left bottom panel of Figure 5. Next the slicing software program converted the shape into a series of slices or layers for printing and finally, a g-code file is then loaded into the printer controller. Each geometry depends on the nozzle size (typically 0.3 or 0.5mm) and how the object is sliced for printing. For example, for hemispherical shells, the slicer prints ring upon ring with decreasing size so that there is less time for the plastic to chill before the next layer is printed. Changing from a 0.5 mm to a 0.3 mm nozzle improves the detail in small printed items and lower nozzle speed reduces problems related to chilling. In our research, good results were obtained for a layer height of 85-90% of the nozzle diameter so that a new layer is lightly squeezed onto the previous layer. The infill density should be set to 100%. A common nontoxic material used in 3D printing is polylactic acid (PLA) with a permittivity of around 2.5 depending on how solid the structure is. The bulk permittivity of a 3D structure depends on how much of it is air and how much of it is PLA. 3D printed structures typically use an algorithm to decide on the lattice enclosed by the outer surface and this needs to be considered during prototyping. Using PLA the authors of [12] have produced a range of structures from solid (2.72+j0.008) to honeycomb (1.24+j0.0002). PLA is therefore relatively low loss.

7. Consideration of Dielectric Loading.

Both the agglomerated powders used in this work and the PLA have low conductivity and can be considered as insulators. Therefore, the conductive elements of an antenna may be placed on top of or within a mixed powder cored 3D printed coating system. A generic dipole was modelled as shown in Figure 6a and Figure 6b.

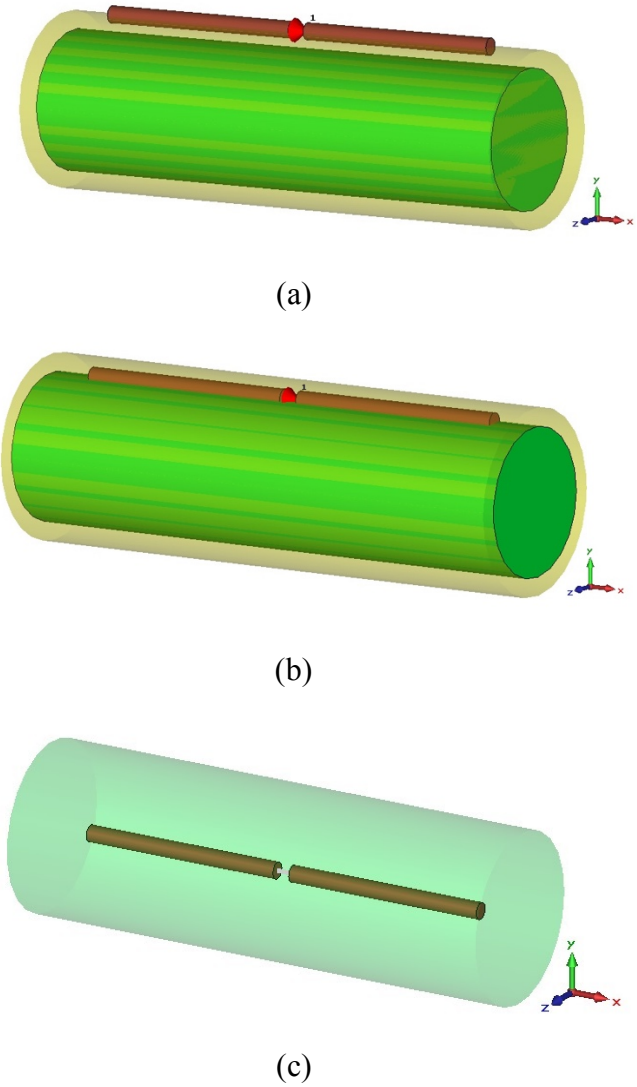

(a)

(b)

(c)

Figure 6. Conductor arrangements of a core a dipole and high permittivity core combination. (a) Conductor on the outer surface, (b) Conductor in the Interface between the core and the PLA shell, (c) Conductor submerged in a core with no coating.

A simple dipole was simulated to illustrate the benefits of a high dielectric coating and test the application of Equation 4 that links the permittivity to the velocity factor on the conducting elements of an antenna.

$$\text{Velocity Factor} = \frac{1}{\sqrt{\varepsilon_r}} \qquad (4)$$

The most effective deployment of the high permittivity material is when the antenna elements are fully immersed and fairly central in the body of the dielectric. This arrangement is shown in Figure 6(c). For a coating of ε_r=7.5 a 2.45 GHz λ/2 dipole was maintained at resonance as the thickness of the coating was increased from 1mm to 60mm Radius. These results are plotted in Figure 7.

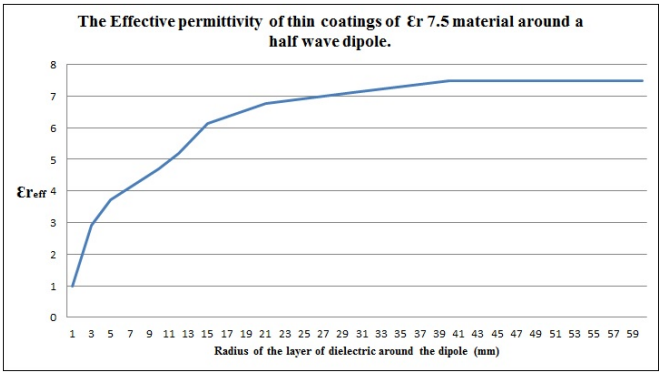

Figure 7. Simulated effects of dielectric coating encasing a resonant half wave dipole at 2.45 GHz.

The results in figure 7 show that reduction in the physical size of the dipole was sub optimal for coverings below approximately λ/2 in thickness and therefore this may be considered the lower bound of Equn. (4) for systems of this type. However, and using this similar technique, higher permittivity dielectrics can be used to compensate for non-optimal coating thickness.

8. Conclusions

A technique for prototyping diectrically loaded antennas (DLAs) has been presented. We have shown how two powders can be combined to produce a complete range of permittivity between 6 to 28. This process can be achieved within the capabilities of most universities.

The novel use of 3D printed forming shells has been introduced which greatly extends the possible applications for DLAs. 3D printing was also used to create a former.

A new type of cavity resonator has been built and combined with a novel 3D printed core. This combination has been shown to be an effective method for characterising the permittivity of low loss mixed agglomerated powders.

Moreover, two relatively readily available candidate powders have been identified and used and a new technique for creating bespoke dielectric fillers has been shown. Since the range of dielectrics is continuous this method lends itself optimisation. The treatment of the materials and methods of measurement can be used to identify other powders and extended to those with magnetic properties. Selection criteria for candidate materials has been provided in this paper. We believe this method will be of particular use for rapid prototyping in research and development as well as for University radio laboratories.

A typical application is in the miniaturisation of existing forms or the prototyping of elements for arrays in limited enclosures such as mobile handsets. In this paper our measurements have been made at room temperature and therefore the stability of these powers at high temperatures has not been investigated. Sintering the mixtures may improve their mechanical properties and allow a reduction in the thickness of the 3D printed shell. Sintering is not required for this method. Other authors have also shown how dielectric coatings can be used to manipulate the size and bandwidth

of antennas although bandwidth was not considered here.

It should be noted, that because of matching, loading an antenna with dielectric is only the first stage of techniques to enhance antenna parameters.

References

[1] H. Nakano, M. Ikeda, K. Hitosugi and J. Yamauchi, "A spiral antenna sandwiched by dielectric layers," in *IEEE Transactions on Antennas and Propagation*, vol. 52, no. 6, pp. 1417-1423, June 2004.

[2] R. Kazemi, A. E. Fathy and R. A. Sadeghzadeh, "Dielectric Rod Antenna Array With Substrate Integrated Waveguide Planar Feed Network for Wideband Applications," in *IEEE Transactions on Antennas and Propagation*, vol. 60, no. 3, pp. 1312-1319, March 2012.

[3] A. A. Kishk, Yan Yin and A. W. Glisson, "Conical dielectric resonator antennas for wide-band applications," in *IEEE Transactions on Antennas and Propagation*, vol. 50, no. 4, pp. 469-474, Apr 2002.

[4] Nelson S.O., 'Measurement and Calculation of Powdered Mixture Permittivities', IEEE Transactions on Instrumentation and Measurement, Vol. 50, No. 5, October 2001.

[5] Minerals water Ltd. http://stores.ebay.co.uk/minerals-water. Both referenced items searched and available 2nd December 2016.

[6] S. O. Nelson and P. G. Bartley, "Open-ended coaxial-line permittivity measurements on pulverized materials," in *IEEE Transactions on Instrumentation and Measurement*, vol. 47, no. 1, pp. 133-137, Feb 1998.

[7] Janezic M. and Baker-Jarvis J., *"Full-wave Analysis of a Split-Cylinder Resonator for Nondestructive Permittivity Measurements,"* IEEE Transactions on Microwave Theory and Techniques vol. 47, no. 10, Oct 1999, pg. 2014-2020

[8] http://www.qwed.com.pl/qmeter.html. Microwave Frequency Q-Meter. Visited Tuesday, 13 February 2018

[9] www.eccosorb.com/Collateral/Documents/English-US/dielectric-chart.pdf. Visited Wednesday, 14 February 2018

[10] R. M. Edwards and G. G. Cook, "3G triband probe fed printed eccentric spiral antenna for nomadic wireless devices using optimal convergence for Pareto ranked genetic algorithm," *2001 Eleventh International Conference on Antennas and Propagation, (IEE Conf. Publ. No. 480)*, Manchester, 2001, pp. 537-541 vol.2. doi: 10.1049/cp:20010345

[11] J. A. Brister and R. M. Edwards, "Design of a balanced ball antenna using a spherical helix wound over a full sphere," *2011 Loughborough Antennas & Propagation Conference*, Loughborough, 2011, pp. 1-4.

[12] Zhang, S et al "Novel 3D printed synthetic dielectric substrates", Microwave and Optical Technology Letters, Vol 57, IS 10